

Crystal-field splitting for low symmetry systems in *ab initio* calculations

S.V. Streltsov,^{1,2} A.S. Mylnikova,^{1,2} A.O. Shorikov,² Z.V. Pchelkina,² D.I. Khomskii,^{3,4} and V.I. Anisimov²

¹*Ural State Technical University, Mira St. 19, 620002 Ekaterinburg, Russia*

²*Institute of Metal Physics, S.Kovalevskoy St. 18, 620219 Ekaterinburg GSP-170, Russia**

³*II. Physikalisches Institut, Universität zu Köln, Zùlpicher Straße 77, D-50937 Köln, Germany*

⁴*Groningen University, Nijenborgh 4, 9747 AG Groningen, The Netherlands*

(Dated: November 14, 2018)

In the framework of the LDA+U approximation we propose the direct way of calculation of crystal-field excitation energy and apply it to La and Y titanates. The method developed can be useful for comparison with the results of spectroscopic measurements because it takes into account fast relaxations of electronic system. For titanates these relaxation processes reduce the value of crystal-field splitting by $\sim 30\%$ as compared with the difference of LDA one electron energies. However, the crystal-field excitation energy in these systems is still large enough to make an orbital liquid formation rather unlikely and experimentally observed isotropic magnetism remains unexplained.

PACS numbers: 71.15.-m, 71.20.-b, 71.30.+h

I. INTRODUCTION

The magnitude of crystal-field splitting (CFS) is known to be very important characteristic of transition metal compounds, necessary for understanding different physical phenomena such as magnetism and metal-insulator transitions.^{1,2} It is often used for detailed fitting of spectroscopic data and in various model calculations. An important question is: how can one calculate CFS in a reliable way?

One can obtain character of CFS using the group theory analysis. It provides qualitative description of ionic levels structure in the presence of crystal-field of given symmetry and can even give some ratios between splittings using Wigner-Eckart theorem.³ However, for quantitative estimates the detailed structure of ionic potentials has to be taken into account.

Generally, there are different contributions to the total value of CFS to be considered. A point-charge contribution can be calculated “by hand” using for instance direct Madelung potential summation (see e.g.⁴). However, this method has some drawbacks and neglects the overlap of the electron clouds of neighboring ions, which can lead to several important consequences.¹

Another important contribution comes from the covalency. It can also be estimated using some model calculations (for instance taking Slater-Koster parameters), but without precise knowledge of the band structure one does not actually know the parameters of the models accurately enough. In order to take into consideration all these contributions to the total value of CFS in a reliable way one should use *ab initio* methods based on density functional theory (DFT) calculations. Nevertheless, even in this case there are several ways to define and calculate CFS. Each of them has its own virtues, but also difficulties.

The first possibility is a direct calculation of the center of gravity of corresponding bands. It works well when splitting is large enough. Thus it is most useful and rather accurate for $t_{2g} - e_g$ splitting (typically in 3d-oxides CFS between t_{2g} and e_g states is $\sim 2-2.5$ eV). For example the behavior of spin-state transition temperature in cobaltites, which depends on this splitting has been recently estimated quite accurately.⁵ The problems might arise in computation of smaller values such as the splitting inside t_{2g} or e_g shells. The general problem is that CFS is a well-defined characteristic only for isolated ions which have energy levels but not bands. The bigger the corresponding band width (in comparison with CFS) the more questionable it becomes to treat the difference of centers of gravity as an estimate of CFS value.

The second way to calculate CFS is the downfolding or projection procedure which could give a few orbital on-site Hamiltonian in the minimal basis set of functions $\psi_1, \psi_2, \dots, \psi_N$.^{6,7} In Sec. IV the method of obtaining such few orbital Hamiltonian from a full orbital one is briefly described.

Having this Hamiltonian one can diagonalize it to obtain its eigenvalues $\epsilon_1, \epsilon_2, \dots, \epsilon_N$ and eigenvectors $\Psi_1, \Psi_2, \dots, \Psi_N$ which are in general linear combinations of the initial wave functions:

$$|\Psi_j\rangle = \sum_i^N a_{ij} |\psi_i\rangle. \quad (1)$$

The eigenvalues can be considered as the energies of the orbitals. The differences between these eigenvalues define in this case CFS.

In spite of great generality of this method, it has some disadvantages. There is an ambiguity in the definition of unitary transformation matrix $U_{ji}^{(\mathbf{k})}$ for Wannier function construction (see Sec. IV) and in the choice of the basis set wave functions $\psi_1, \psi_2, \dots, \psi_N$ in any downfolding or projection procedure. Using different basis sets few orbital non-interacting Hamiltonian can be constructed in different ways. All of them are equally good if the resulting Hamiltonian gives the same bands as the LDA full orbital one. It is essentially important for low symmetry systems, where it is not clear what kind of linear combinations of d -wave functions and in which local coordinate system (LCS) should be taken as a basis set for few orbital Hamiltonian construction.

In addition there is one more serious and general problem. LDA calculations are widely known to give good description of the *ground state* characteristics. However, it often fails to describe the excited states. LDA eigenvalues should not be treated as the real excitation energies. This general shortcoming concerns all methods of calculating CFS which use LDA eigenvalues.

On the other hand, care should be taken in what we actually mean by CFS. In direct study of CF excitations e.g. by optics one should take into account possible relaxation of both the electronic (fast process) and lattice (relatively slow relaxation) subsystems. Fast electronic relaxation definitely has to be taken into consideration, whereas the lattice relaxation can be often treated separately (direct optical absorptions usually occur at a frozen lattice, according to the Frank-Condon principle).

In this paper we propose *the direct method* of calculation of CF excitation energy in the framework of the LDA+U approximation which allows for such relaxation of electron system and enables to avoid ambiguity in the choice of basis set (as in projection or downfolding procedure) as well. CF excitations are calculated as difference between the ground state energy and the total energy of an excited state in which the electron is “artificially” put to one of the higher-lying d -levels. These states - the ground state and the excited state with the electron constrained in the higher level - are both treated in the self-consistent LDA+U scheme. This allows us to obtain the values of CF excitation energy which, in particular, take into account fast relaxation of the electronic system.

Below we develop this general method and test it on the example of Y and La titanates. We compare our results with the previously obtained ones.^{8,9} The physics of these compounds is discussed on the basis of calculated values of CF excitation energy, as well as the other results of *ab initio* LDA and LDA+U calculations.

II. PHYSICS OF TITANATES AND CRYSTAL-FIELD SPLITTING

Unusual and very rich physics of titanates attracts much attention since the possibility of existence of an orbital liquid has been proposed for LaTiO_3 .^{10,11} In the ground state both LaTiO_3 and YTiO_3 crystallize in perovskite structure. The lattice distortions due to different ionic radii of Y and La ions seems to lead to the cardinal changes in electronic and magnetic properties of these compounds.

At low temperatures LaTiO_3 was found to be G-type antiferromagnet with Néel temperature for stoichiometric samples $T_N=146 \text{ K}$ while YTiO_3 is an isotropic ferromagnet with relatively low $T_C \sim 30 \text{ K}$.¹² Local magnetic moment on Ti^{3+} ion in YTiO_3 was found to be $0.84 \mu_B$.¹² The ordered moment in LaTiO_3 amounts to $0.46 - 0.58 \mu_B$ ^{4,10,13} and strongly differs from $1 \mu_B$ expected for d^1 configuration with quenched orbital moment. Another interesting feature is nearly isotropic magnon spectra with small spin gap observed both in LaTiO_3 and YTiO_3 despite of the intrinsic orthorhombic distortion.^{10,14}

In order to describe these puzzling properties the exciting idea of the orbital liquid has been proposed.¹¹ According to this theory the large degeneracy of t_{2g} shell can lead to the orbitally-disordered ground state. The crucial point in this case is the value of energy required for electron excitation from one t_{2g} orbital to another: orbital liquid can exist only if this energy is zero or very small.

However, as the real symmetry of LaTiO_3 and YTiO_3 is not cubic but orthorhombic, one should expect certain splitting of t_{2g} -levels. First calculations of the CFS in LaTiO_3 was performed by R. Schmitz and E. Müller-Hartmann.^{4,15} Using realistic crystal structure⁴ they carried out model calculations taking into account point-charge and covalency contributions and obtained that the lowest singlet is separated from two higher-lying almost degenerate levels by about 0.24 eV. Similar calculations were also performed by Mochizuki and Imada.¹⁶ They stressed the importance of the GdFeO_3 -type distortion and found the value of CFS to be $0.77/\epsilon_{\text{TiLa}}$ eV, where ϵ_{TiLa} is an effective dielectric constant. This constant is hard to evaluate in model calculations in a reliable way because of local screening effects in a solid, which could be explicitly taken into account only in *ab initio* band structure calculations.

The *ab initio* calculations were done by Pavarini *et al.*⁸ and Solovyev.⁹ They used the diagonalization of few orbital on-site effective LDA Hamiltonian in real space to obtain CFS. Solovyev has performed an exact procedure of full-orbital Hamiltonian transformation to the small energy-dependent Hamiltonian. After that the energy

was fixed in the center of the t_{2g} band.⁹ Pavarini *et al.*⁸ have used formalism of Nth-order muffin-tin orbitals (NMTOs) to define small Hamiltonian.⁶ Despite the similarity of the methods, the results are qualitatively different. The CFS

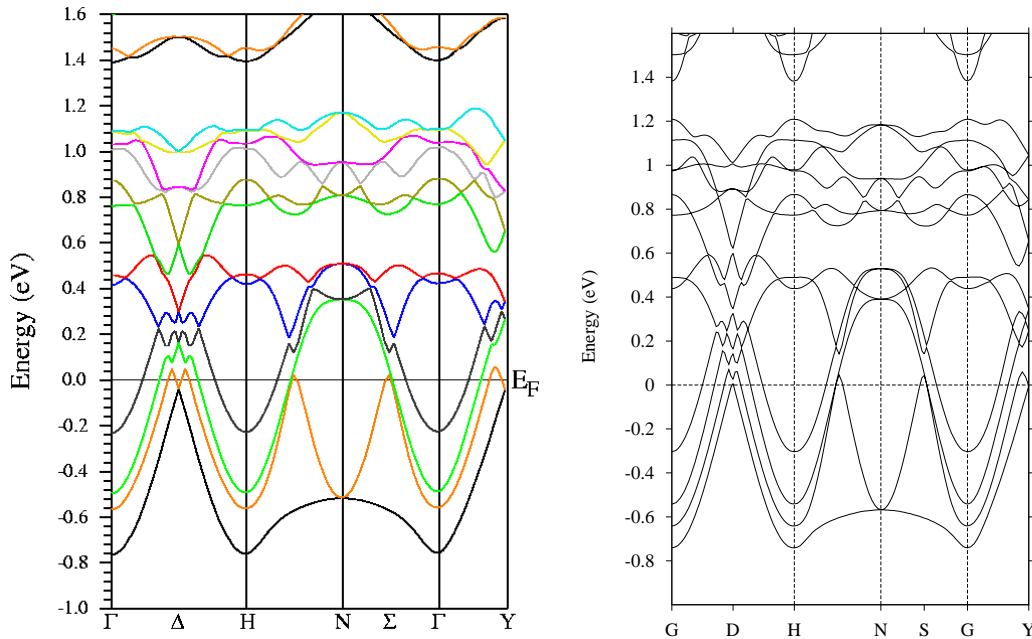


FIG. 1: (color online) Band structure for LaTiO_3 obtained within the LDA approximation in the framework of two methods: the full potential linearized augmented plane waves – FP-LAPW (left) and linear muffin-tin orbitals – LMTO (right). The energy region is chosen to illustrate the behavior of t_{2g} bands. The Fermi level corresponds to zero energy.

between lowest and next t_{2g} level obtained in Ref. 9 is rather small, $\sim 30\text{-}50$ meV for both compounds, which would not prevent an orbital liquid formation. However, the results of calculations presented in Ref. 8 are incompatible with this scenario: obtained values of CFS are $\sim 150\text{-}200$ meV for both compounds, similar to the results of model calculations.^{4,16}

III. LDA: BAND STRUCTURE

Discrepancy between the results of previous *ab initio* CFS calculations^{8,9} is probably caused by (i) choice of MT spheres radii in LMTO method¹⁷ or (ii) the details of different projection procedures. To resolve first problem we have carried out the conventional LDA calculations using LMTO method and verified its band structure by performing the full-potential calculations in the framework of linearized augmented plane waves (FP-LAPW) method realized on Wien2k program code.¹⁸ We chose FP-LAPW because it is known to be the most accurate method for band structure calculations.

Crystallographic data for LaTiO_3 ($T=8$ K) and YTiO_3 ($T=293$ K) were taken from Ref. 4. The radii of the muffin-tin (MT) spheres for LMTO calculations were chosen to be $R_{\text{La}}=3.28$ a.u., $R_{\text{Ti}}=2.52$ a.u., and for both oxygens $R_{\text{O}}=1.92$ a.u. Remaining unit cell volume was filled by empty spheres (atomic spheres with zero nuclear charge) with different MT radii. Ionic radius of Y is known to be smaller than La one.¹⁹ According to this fact the MT radius of Y was also taken to be smaller: $R_{\text{Y}}=3.01$ a.u.

The $\text{Ti}(4s,4p,3d)$, $\text{O}(3s,2p,3d)$ and $\text{Y}(5s,5p,4d,4f)$, $\text{La}(6s,6p,5d)$ states were included in the basis set in our calculations. Almost empty $\text{La-}4f$ states were treated as pseudo-core, since $\text{La-}4f$ states are localized and do not strongly contribute to the relevant electronic states. Due to rather large values of the on-site Coulomb interaction U (of the order of 10 eV) $\text{La-}4f$ states will be located approximately at 5-10 eV above the Fermi level.²⁰

The Brillouin-zone (BZ) integration in the course of the self-consistent iterations was performed over a mesh of 27 \mathbf{k} -points in the irreducible part of the BZ. Density of states (DOS) were calculated by the tetrahedron method with 512 \mathbf{k} -points in the whole BZ.

The band structure obtained within the LDA approximation in the framework of LMTO (with the MT radii chosen above) and FP-LAPW methods for LaTiO_3 is presented in Fig. 1. Twelve $\text{Ti-}t_{2g}$ (four Ti per unit cell) bands are placed in the vicinity of the Fermi level and have band width ~ 1.95 eV both in FP-LAPW and LMTO methods. The energy gap between the top of the t_{2g} and the bottom of e_g bands is estimated to be 0.25 eV in FP-LAPW and

0.18 eV in LMTO. Comparing this figure and Fig. 2 of Ref. 9 one can see that the present LMTO bands agree better in all high-symmetry points of BZ with FP-LAPW ones than those presented in Ref. 9. So being firmly convinced of the correctness of LMTO band structure one could carry out the CFS calculations.

IV. LDA: WANNIER FUNCTION PROJECTION FOR CRYSTAL-FIELD SPLITTING CALCULATION

One of the ways to calculate CFS is to use the minimal basis set Hamiltonian for the orbitals of interest in real space. To construct such Hamiltonian we used Wannier functions projection procedure. In this section we present brief description of the method. For more details, see Ref. 7.

For an LDA Hamiltonian \hat{H} one has a Hilbert space of eigenfunctions (Bloch states $|\psi_{i\mathbf{k}}\rangle$) with the basis set $|\phi_\mu\rangle$ defined by the particular method (for LMTO these are LMT-orbitals,¹⁷ for LAPW - Augmented Plane Waves,²¹ etc.). In this basis set the Hamiltonian operator is defined as:

$$\hat{H} = \sum_{\mu\nu} |\phi_\mu\rangle H_{\mu\nu} \langle\phi_\nu|, \quad (2)$$

where greek indices are used for full-orbital matrices.

If we consider a certain subset of the Hamiltonian eigenfunctions, for example Bloch states of partially filled bands $|\psi_{n\mathbf{k}}\rangle$, then we can define a corresponding subspace in the total Hilbert space. The Hamiltonian matrix is diagonal in the Bloch states basis, however, physically more appealing is a basis which would have a form of site-centered atomic orbitals. That is a set of Wannier functions $|W_n^{\mathbf{T}}\rangle$ defined as a Fourier transformation of certain linear combination of Bloch functions belonging to this subspace (see Eq. (4) below). They are labeled in real space according to the band n and the lattice vector of the unit cell \mathbf{T} which they belong to. The Hamiltonian operator \hat{H}^{WF} defined in this basis set is

$$\hat{H}^{WF} = \sum_{nn'\mathbf{T}} |W_n^0\rangle H_{nn'}(\mathbf{T}) \langle W_{n'}^{\mathbf{T}}|. \quad (3)$$

The total Hilbert space can be divided into a direct sum of above introduced subspace (of partially filled Bloch states) and the subspace formed by all other states orthogonal to it. Those two subspaces are decoupled since they are the eigenfunctions corresponding to different eigenvalues. The Hamiltonian matrix in Wannier function basis is block-diagonal, so that the matrix elements between different subspaces in Hilbert space are zero. The block $H_{nn'}$ in (3) corresponding to the partially filled bands can be considered as a projection of the full Hamiltonian operator (2) to the subspace defined by its Wannier functions.

Localized Wannier functions $|W_i^{\mathbf{T}}\rangle$ were defined in Ref. 22 as Fourier transforms of the Bloch functions $|\psi_{i\mathbf{k}}\rangle$

$$|W_i^{\mathbf{T}}\rangle = \frac{1}{\sqrt{N}} \sum_{\mathbf{k}} e^{-i\mathbf{k}\mathbf{T}} |\psi_{i\mathbf{k}}\rangle, \quad (4)$$

where N is the number of discrete \mathbf{k} points in the first BZ.

Wannier functions are not uniquely defined because for a certain set of bands any orthogonal linear combination of Bloch functions $|\psi_{i\mathbf{k}}\rangle$ can be used in (4). In general it means that the freedom of choice of Wannier functions corresponds to freedom of choice of a \mathbf{k} -dependent unitary transformation matrix $U_{ji}^{(\mathbf{k})}$:²³

$$|\tilde{\psi}_{i\mathbf{k}}\rangle = \sum_j U_{ji}^{(\mathbf{k})} |\psi_{j\mathbf{k}}\rangle. \quad (5)$$

The most serious drawback of Wannier representation is that there is no rigorous way to define $U_{ji}^{(\mathbf{k})}$. As one can see from (4) and (5), Wannier functions can vary significantly in shape and range because variations in $|\psi_{i\mathbf{k}}\rangle$ or $U_{ji}^{(\mathbf{k})}$ change relative phases and amplitudes of Bloch functions at different \mathbf{k} and bands i .

In order to avoid this disadvantage some additional restrictions on the properties of Wannier functions have been proposed.^{23,24,25} Among others Marzari and Vanderbilt²³ suggested the condition of maximum localization for Wannier functions. That gave the variational procedure to calculate $U_{ji}^{(\mathbf{k})}$. To get a good initial point the authors suggested to choose a set of trial localized orbitals $|\phi_n\rangle$ and projecting them onto the Bloch functions $|\psi_{i\mathbf{k}}\rangle$. It was found that this starting guess is usually quite good.²³ This fact led later to the simplified calculating scheme proposed in²⁶ where variational procedure was abandoned and the result of aforementioned projection was considered as a final step.

TABLE I: The magnitudes of CFS in t_{2g} shell (in meV) obtained in the LDA approach by different authors are presented in first 3 columns. First value is an energy difference between the lowest energy level and the middle one; the second is the difference between the middle and the highest energy levels in t_{2g} shell. The results of the constrained LDA+U calculations, which take into account fast electron relaxations are shown in the last column.

	Present results (WF projection)	E. Pavarini <i>et al.</i> ^a	I.V. Solovyev ^b	Present results (LDA+U)
<i>LaTiO</i> ₃	230; 40	140; 60	54; 39	160; -
<i>YTiO</i> ₃	180; 80	200; 130	27; 154	150; -

^aReference⁸

^bReference⁹

In order to start projection procedure one needs to determine the set of trial orbitals $|\phi_n\rangle$ and the bands which will be used for the Wannier functions construction. The latter can be defined either by the bands numbers (from N_1 to N_2) or by the energy interval (E_1, E_2) .

Non-orthogonalized Wannier functions in real $|\widetilde{W}_n^{\mathbf{T}}\rangle$ and reciprocal space $|\widetilde{W}_{n\mathbf{k}}\rangle$ are then the projection of the set of trial site-centered atomic-like orbitals $|\phi_n\rangle$ on the Bloch functions $|\psi_{i\mathbf{k}}\rangle$ of the chosen bands

$$|\widetilde{W}_n^{\mathbf{T}}\rangle = \frac{1}{\sqrt{N}} \sum_{\mathbf{k}} e^{-i\mathbf{k}\mathbf{T}} |\widetilde{W}_{n\mathbf{k}}\rangle, \quad (6)$$

$$|\widetilde{W}_{n\mathbf{k}}\rangle \equiv \sum_{i=N_1}^{N_2} |\psi_{i\mathbf{k}}\rangle \langle \psi_{i\mathbf{k}} | \phi_n \rangle = \sum_{i(E_1 \leq \varepsilon_i(\mathbf{k}) \leq E_2)} |\psi_{i\mathbf{k}}\rangle \langle \psi_{i\mathbf{k}} | \phi_n \rangle.$$

Note that the Wannier functions in reciprocal space $|\widetilde{W}_{n\mathbf{k}}\rangle$ do not coincide with the Bloch functions $|\psi_{n\mathbf{k}}\rangle$ for multi-band case due to the summation over band index i in (6). One can consider them as Bloch sums of Wannier functions analogous to the basis functions Bloch sums $\phi_{\mu}^{\mathbf{k}}(\mathbf{r})$, see (8) below.

The coefficients $\langle \psi_{i\mathbf{k}} | \phi_n \rangle$ in (6) define (after orthonormalization) the unitary transformation matrix $U_{ji}^{(\mathbf{k})}$ in (5). However, projection procedure defined in (6) can be considered as a more general formalism than unitary transformation (5).

The Bloch functions in LMTO basis take the form

$$|\psi_{i\mathbf{k}}\rangle = \sum_{\mu} c_{\mu i}^{\mathbf{k}} |\phi_{\mu}^{\mathbf{k}}\rangle, \quad (7)$$

where μ is the combined index of the qlm (q - atomic number in the unit cell, lm are orbital and magnetic quantum numbers), and $\phi_{\mu}^{\mathbf{k}}(\mathbf{r})$ are Bloch sums of the basis orbitals $\phi_{\mu}(\mathbf{r} - \mathbf{T})$

$$\phi_{\mu}^{\mathbf{k}}(\mathbf{r}) = \frac{1}{\sqrt{N}} \sum_{\mathbf{T}} e^{i\mathbf{k}\mathbf{T}} \phi_{\mu}(\mathbf{r} - \mathbf{T}), \quad (8)$$

and the coefficients have the property $c_{\mu i}^{\mathbf{k}} = \langle \phi_{\mu} | \psi_{i\mathbf{k}} \rangle$.

If n in $|\phi_n\rangle$ corresponds to the particular qlm combination (in other words $|\phi_n\rangle$ is an *orthogonal* LMTO basis set orbital), then $\langle \psi_{i\mathbf{k}} | \phi_n \rangle = c_{ni}^{\mathbf{k}*}$ and hence

$$\begin{aligned} |\widetilde{W}_{n\mathbf{k}}\rangle &= \sum_{i=N_1}^{N_2} |\psi_{i\mathbf{k}}\rangle c_{ni}^{\mathbf{k}*} \\ &= \sum_{i=N_1}^{N_2} \sum_{\mu} c_{\mu i}^{\mathbf{k}} c_{ni}^{\mathbf{k}*} |\phi_{\mu}^{\mathbf{k}}\rangle = \sum_{\mu} \tilde{b}_{\mu n}^{\mathbf{k}} |\phi_{\mu}^{\mathbf{k}}\rangle, \\ \tilde{b}_{\mu n}^{\mathbf{k}} &= \sum_{i=N_1}^{N_2} c_{\mu i}^{\mathbf{k}} c_{ni}^{\mathbf{k}*}. \end{aligned} \quad (9)$$

In order to orthonormalize the WF (9) an overlap matrix $O_{nn'}(\mathbf{k})$ and its inverse square root $S_{nn'}(\mathbf{k})$ can be defined as

$$O_{nn'}(\mathbf{k}) \equiv \langle \widetilde{W}_{n\mathbf{k}} | \widetilde{W}_{n'\mathbf{k}} \rangle = \sum_{i=N_1}^{N_2} c_{ni}^{\mathbf{k}} c_{n'i}^{\mathbf{k}*}, \quad (10)$$

$$S_{nn'}(\mathbf{k}) \equiv O_{nn'}^{-1/2}(\mathbf{k}),$$

The orthogonality of Bloch states $\langle \psi_{n\mathbf{k}} | \psi_{n'\mathbf{k}} \rangle = \delta_{nn'}$ was used.

Orthonormalized Wannier functions in k -space $|W_{n\mathbf{k}}\rangle$ can be obtained as

$$\begin{aligned} |W_{n\mathbf{k}}\rangle &= \sum_{n'} S_{nn'}(\mathbf{k}) |\widetilde{W}_{n'\mathbf{k}}\rangle = \sum_{i=N_1}^{N_2} |\psi_{i\mathbf{k}}\rangle \bar{c}_{ni}^{\mathbf{k}*} \\ &= \sum_{\mu} b_{\mu n}^{\mathbf{k}} |\phi_{\mu}^{\mathbf{k}}\rangle, \end{aligned} \quad (11)$$

where

$$\bar{c}_{ni}^{\mathbf{k}*} \equiv \langle \psi_{i\mathbf{k}} | W_{n\mathbf{k}} \rangle = \sum_{n'} S_{nn'}(\mathbf{k}) c_{n'i}^{\mathbf{k}*}, \quad (12)$$

$$b_{\mu n}^{\mathbf{k}} \equiv \langle \phi_{\mu}^{\mathbf{k}} | W_{n\mathbf{k}} \rangle = \sum_{i=N_1}^{N_2} \bar{c}_{\mu i}^{\mathbf{k}} \bar{c}_{ni}^{\mathbf{k}*}. \quad (13)$$

Thus, matrix elements of the few orbital Hamiltonian \hat{H}^{WF} in the basis of WF in real space where both orbitals are in the same unit cell are given by the following expression

$$\begin{aligned} H_{nm}^{WF}(0) &= \langle W_n^{\mathbf{0}} | \frac{1}{N} \left(\sum_{\mathbf{k}} \sum_{i=N_1}^{N_2} |\psi_{i\mathbf{k}}\rangle \epsilon_i(\mathbf{k}) \langle \psi_{i\mathbf{k}}| \right) | W_m^{\mathbf{0}} \rangle = \\ &= \frac{1}{N} \sum_{\mathbf{k}} \sum_{i=N_1}^{N_2} \bar{c}_{ni}(\mathbf{k}) \bar{c}_{mi}^*(\mathbf{k}) \epsilon_i(\mathbf{k}). \end{aligned} \quad (14)$$

Here $\epsilon_i(\mathbf{k})$ is an eigenvalue for a particular band.

For both LaTiO_3 and YTiO_3 we are interested in CFS in the t_{2g} shell. For that 3×3 Hamiltonians were derived for t_{2g} bands placed in the vicinity of the Fermi level in the energy range (-0.8; 1.25) eV for LaTiO_3 and (-0.65; 1.55) eV for YTiO_3 . Then we diagonalize them and calculate the difference between corresponding eigenvalues in order to determine the CFS.

The obtained values of CFS together with results of Ref. 8,9 are presented in Tab. I. The CFS calculated by Pavarini *et al.*⁸ has the same character and similar values as ours. According to these results, in LaTiO_3 the lowest energy level is widely separated from two other, which are almost degenerate. Similar result was obtained by Cwik *et al.* using a full Madelung-sum point charge model, where the first splitting was found to be 240 meV.⁴

The situation is a little bit different in YTiO_3 . The magnitude of the first splitting (between lowest and middle energy levels) has the same order as in La titanate, while the second one (between middle and highest energy levels) increases. It is interesting to note that in calculations of Solovyev the same effect of the second splitting enhancement going from LaTiO_3 to YTiO_3 is observed.⁹ Nevertheless, the character of CFS obtained by Solovyev⁹ is quite different from the present one and from that calculated in Ref. 8.

V. LDA+U: BAND STRUCTURE

The application of LDA to solids provides important information about details of band structure. However, for transition metal compounds it usually leads to metallic type of the electronic structure due to the presence of the partially filled d -bands at the Fermi level, often in contrast with an experiment. This is also the case in the LDA approach presented above (Sec. IV). The LDA+U approximation has been developed to include in the calculation scheme orbital-dependent Hubbard-like correction U which acts differently on the occupied and unoccupied d -orbitals giving as a result correct description for localized states.²⁷

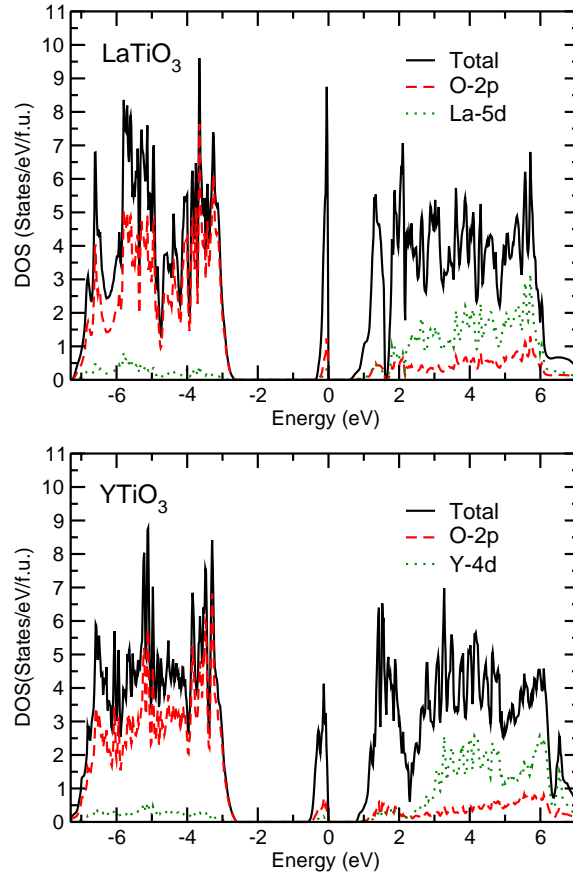


FIG. 2: (color online). Total and partial DOS of LaTiO_3 (top panel) and YTiO_3 (bottom panel) calculated within the LDA+U approximation for AFM-G and FM magnetic structures, respectively. The Fermi level corresponds to zero energy.

In order to analyze the results of the LDA+U calculations in terms of t_{2g} and e_g orbitals one has to choose in the local coordinate system (LCS). Usually it is possible to define the LCS where axes are pointed directly along $Ti-O$ bonds, but for strongly distorted compounds (like LaTiO_3 and YTiO_3) such coordinate system in general might be not rectangular. We use the rectangular local coordinate system where the axes are directed as much as possible to the nearest oxygens.

The interorbital on-site Coulomb interaction parameter U and intra-atomic exchange coupling J for t_{2g} shell were estimated to be 3.3 eV and 0.8 eV, respectively, using constrained superscell calculations²⁸ in the framework of LMTO method and taking into account screening by e_g electrons.²⁹ These values are in good agreement with previous findings.^{29,30} The experimentally observed magnetic structures: YTiO_3 - ferromagnet, LaTiO_3 - G-type antiferromagnet are used for the conventional and constrained LDA+U calculations.

The top panel of Fig. 2 shows LDA+U electronic structure of LaTiO_3 in details. There are three distinguishable sets of bands: completely filled O-2p bands, partially filled Ti-3d bands and empty La-5d bands. The bands in the energy range from -7.2 eV to -2.7 eV originate mainly from O-2p states. The gap ~ 2.3 eV appears between O-2p and the narrow peak of Ti-3d(t_{2g}) states. The band gap in LaTiO_3 is found to be 0.57 eV. It divides Ti-3d(t_{2g}) band into two parts in such a way that both the top of the valence and the bottom of the conduction band are predominantly formed by Ti-3d(t_{2g}) states (see Fig. 3). The bands lying higher than ~ 2 eV have basically La-3d, O-2p and Ti-3d(e_g) contributions. The calculated local magnetic moment on Ti^{3+} ion amounts to $0.78\mu_B$ being by $\sim 0.2\mu_B$ larger than the experimentally observed value.⁴

The electronic structure obtained in the LDA+U approximation for YTiO_3 is shown in the bottom panel of Fig. 2. Generally it has similar character. However, the value of the band gap is larger than in LaTiO_3 (~ 0.78 eV). The value of the local magnetic moment is found to be $0.89\mu_B$ in good agreement with experiment.¹²

There are two opposite factors influencing the magnitude of the band gap. On one hand the larger lattice distortions in YTiO_3 due to smaller ionic radii of Y in comparison with La make Ti(3d)-O(2p) hybridization weaker and as a

TABLE II: Total energy difference between three magnetic solutions per Ti ion and magnitudes of the band gaps and local magnetic moments on Ti ions obtained in LDA+U calculation. Zero energy is the lowest total energy for compound under consideration.

	<i>LaTiO₃</i>			<i>YTiO₃</i>		
	Band gap	Mag. moment	Total energy	Band gap	Mag. moment	Total energy
FM	0.45 eV	0.88 μ_B	125 K	0.78 eV	0.89 μ_B	0
AFM-A	0.54 eV	0.83 μ_B	0	0.89 eV	0.87 μ_B	60 K
AFM-G	0.57 eV	0.78 μ_B	40 K	1.04 eV	0.81 μ_B	230 K

result the band gap larger. On the contrary, ferromagnetism observed in $YTiO_3$ leads to an increase of the band width resulting in a band gap reduction.

In order to clarify the role of magnetism we performed additional band structure calculations for magnetic structures different from experimental one.

The FM, AFM-G and AFM-A structures were considered. The values of the band gap and local magnetic moments on Ti^{3+} ions for all calculated configurations are presented in Tab. II. One can see that the band gap reduction due to ferromagnetism amounts to 21% (0.12 eV) in the case of $LaTiO_3$ and 25% (0.26 eV) in $YTiO_3$. The modifications of an electronic structure with the change of magnetic structure from AFM-G to FM in the vicinity of Fermi level for $LaTiO_3$ are presented in the inset of Fig.3.

Continuing investigation of the interplay between lattice, electronic and magnetic degrees of freedom one can isolate the influence of “pure lattice distortions” on the electronic structure of La and Y titanates comparing the results of calculations performed in identical magnetic structures. The analysis shows significant changes in the value of the band gap. Only due to the lattice distortions it changes by 0.32-0.47 eV depending on the magnetic structure under consideration.

The main reason for such a strong influence of local geometry on the electronic structure of these compounds is probably connected with the stronger covalency of d^1 configuration and hence higher sensibility to the distortions in comparison with other configurations of d -shell (with the exclusion of d^9). In contrast to the band gap, magnetic moment is only reduced by 10% with the change of magnetic configuration.

In addition, it should be mentioned that our calculations unlike the experiment give for $LaTiO_3$ the lowest total energy for A-type AFM, although experimentally observed G-type lies quite close. This result is supported by the calculation of the exchange interaction parameters⁹ and connected with the orbital pattern of the compound discussed in details in Sec. VII.

VI. CALCULATION OF CRYSTAL-FIELD EXCITATION ENERGY IN LDA+U

The direct study of CFS, for instance by optical measurements, implies the excitation of an electron from one energy level to another. Simultaneously with this excitation the external “bath” formed by the rest of the electrons can relax giving the system a chance to lower the energy. The simple CFS computations using the centers of gravity of corresponding bands, projection or downfolding procedure do not take into account such processes and as a result overestimate the value of CFS. In this section we propose the direct calculation of the total energy difference between ground and first excited states (*CF excitation energy calculation*) in t_{2g} shell using the constrain procedure adopted for the LDA+U approximation.

The occupation matrix in LDA+U can be defined in the usual way:

$$n_{mm'}^\sigma = -\frac{1}{\pi} \int^{E_F} \text{Im} G_{inlm, inlm'}^\sigma(E) dE, \quad (15)$$

where σ is the spin, i denotes the site, n, l, m are principle, orbital and magnetic quantum numbers respectively, $G_{inlm, inlm'}^\sigma(E) = \langle inlm\sigma | (E - \hat{H}^{LDA+U})^{-1} | inlm'\sigma \rangle$ are the elements of the Green function matrix and \hat{H}^{LDA+U} is a single particle LDA+U Hamiltonian (for its definition see Ref. 27). The occupation matrix for an isolated ion is diagonal. However, for ions in solids it can have more complex structure in low symmetry systems and one needs to diagonalize it. The eigenvectors of the (15) can be used for transformation of occupation matrix to diagonal form. Using this procedure one can obtain the information on the orbitals where the electrons are localized.

In fact, in the case of spin-polarized calculations (like LDA+U) there are two occupation matrices for every transition metal ion on each site: spin majority and spin minority occupation matrices. According to the Hund's rule, at first the spin majority states start to be occupied. Nevertheless, due to the large spatial extension and sizable overlap between e_g and oxygen p orbitals (see Fig. 3) there are always some non-negligible occupation numbers for e_g states in a real band structure calculation for both spins. In order to avoid the influence of these effects (they can lead to the “symmetrization” of d -orbitals) we use for the analysis not the occupation matrix for majority spin (Ti is d^1 system in the compounds under consideration), but the difference between matrices for two spins. Here we suppose the oxygen influence on d -states for both spins to be equal.

The diagonalization of the difference between occupation matrices for majority and minority spins for LaTiO_3 gives following eigenvalues: 0, 0, 0.01, 0.02, 0.76. The eigenvector corresponding to the largest eigenvalue defines the occupied orbital as a linear combination of all d -orbitals:

$$|\Psi_{GS}\rangle = \sum_i a_i |\psi_i\rangle. \quad (16)$$

Thus, in case of LaTiO_3 in the LCS:

$$|\Psi_{GS}^{LaTiO_3}\rangle = 0.62xy + 0.72yz + 0.32xz + 0.02(3y^2 - r^2) + 0.02(z^2 - x^2). \quad (17)$$

Similar decomposition for YTiO_3 is presented in the Table III.

The excitation energy (from the ground to the first excited state) in this case is the total energy difference between states where this orbital is occupied and where it is empty and another one is occupied. According to this scheme we performed the calculation where the system is constrained by external potential \hat{V}_{constr} to change the occupied orbital:

$$\hat{V}_{constr} = |\Phi_{GS}\rangle \delta V \langle \Phi_{GS}|. \quad (18)$$

In other words \hat{V}_{constr} just pushes up the orbital where the electron has been localized in LDA+U. It is not important how big is the correction δV . One needs just be sure that it is large enough to force the electron to hop to another orbital. The total energy of excited state does not depend on the value of δV , because the correction is applied to the orbital which has to be empty in the excited state. The total energy difference between the ground and first excited states is an estimate of the CF excitation energy.

The results of calculations of CF excitation energies for LaTiO_3 and YTiO_3 are presented in the fourth column of Tab. I. They have the same order of magnitude as those obtained using the WF projection in the present work and downfolding performed by Pavarini *et al.*⁸ As has been mentioned above, for proper estimation of CF excitation energy the relaxation of electron system should be taken into consideration. Such relaxation decreases the energy costs of the electron excitation. According to the present results the gain in energy can amount to ~ 70 meV ($\sim 30\%$). However, it is obviously insufficient to reduce the value of CFS significantly.

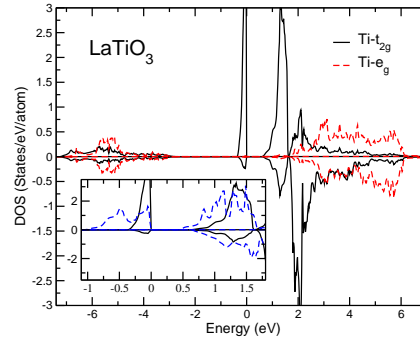


FIG. 3: (color online). LaTiO_3 . Ti-3d partial DOS calculated within LDA+U approach. The inset shows Ti-3d partial DOS in AFM-G (solid line) and FM (dashed line) configurations. Parts of plots with positive (negative) ordinates denote majority (minority) spin DOS. The Fermi level corresponds to zero energy.

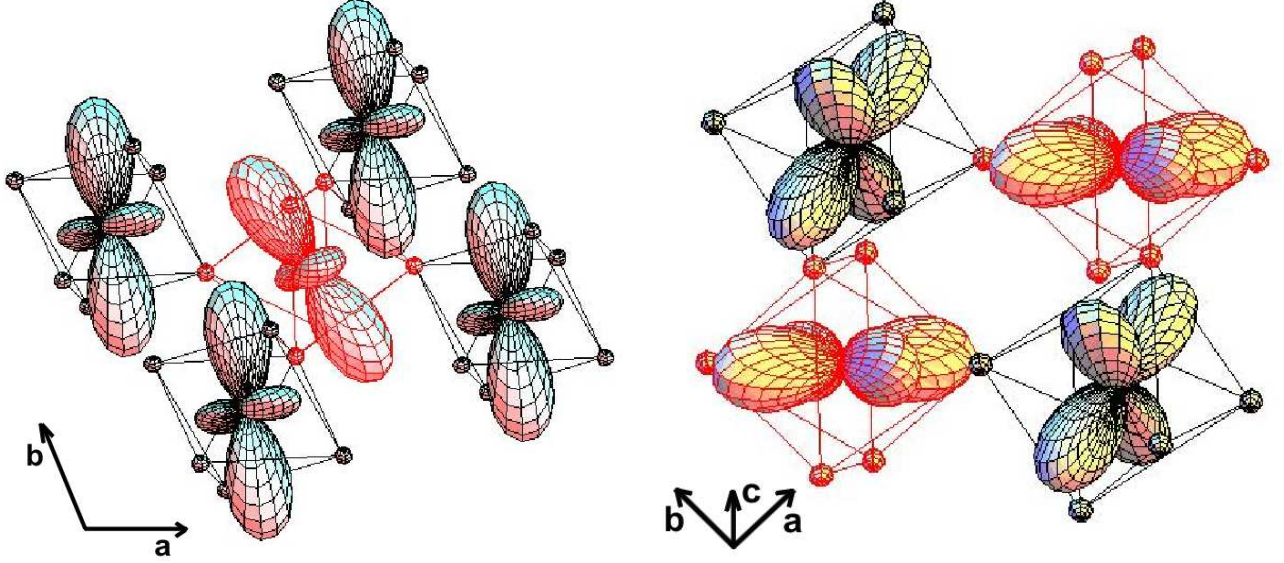


FIG. 4: (color online) Orbital ordering in LaTiO_3 (left) and YTiO_3 (right) in ab -plane obtained in the framework of the LDA+U calculations for AFM-G and FM structures respectively.

Thus, the results of the CFS calculations both using WF projection and constrained LDA+U which takes into account the electron system relaxation indicate that the splittings in LaTiO_3 and YTiO_3 are relatively large. They are definitely bigger than the spin-orbital coupling in titanates which is expected to be $\Lambda_{SO} \sim 20 \text{ meV}$ ³¹. The latter result is supported by the recent XAS measurements, where shown that the orbital momentum in LaTiO_3 is essentially quenched.³²

But the most important conclusion is that CF excitation energy obtained in the present work and value of CFS calculated in Ref. 8 as well as extracted from Ti $L_{2,3}$ XAS³² and optical measurements³³ are all the order of 200 meV, that makes orbital liquid scenario for LaTiO_3 rather unlikely.

VII. ORBITAL STRUCTURE

Orbital degrees of freedom are known to play an important role and should be correctly taken into account in theories describing magnetic interactions in strongly correlated materials.³⁴

As one can see from Tab. III the composition of the occupied orbitals in Y and La titanates is quite different. Contribution of xy and yz components to the resulting orbital in LaTiO_3 are nearly the same and by $\sim 40\text{--}60\%$ bigger than xz one. There is quite different situation in YTiO_3 , where xz contribution is almost zero.

This fact can be explained by means of the analysis of the crystal structure distortions, which are quite different in these compounds. Distortions in ab -plane in LaTiO_3 have in general large trigonal D_{3d} component. It gives rise to square-to-rectangle transformation in this plane⁴ and results in localization of the electron on the orbital of almost $a_{1g} = (xy + yz + zx)/\sqrt{3}$ character. At the same time the predominant distortions in YTiO_3 make rhombus from the initial square, revealing the sizable contribution of local tetragonal distortions.

TABLE III: Decomposition of the lowest in energy orbital into xy , xz and yz orbitals. The results are presented in local coordinate system where the orthogonal axes point as much as possible to neighboring oxygens.

	LaTiO_3	YTiO_3
LDA	$0.63xy + 0.66yz + 0.40xz$	$0.76xy + 0.64yz - 0.06xz$
LDA+U	$0.62xy + 0.72yz + 0.32xz$	$0.75xy + 0.66yz - 0.04xz$

However, even in case of LaTiO_3 the occupied orbital deviates from a_{1g} :

$$|\langle \Psi_{LDA+U} | a_{1g} \rangle|^2 = 91\% \quad (19)$$

$$|\langle \Psi_{LDA} | a_{1g} \rangle|^2 = 96\% \quad (20)$$

The variation of $Ti - O$ distances in YTiO_3 ³⁵ leads to antiferroorbital ordering (Fig. 4,5) inducing according to Goodenough-Kanamori rules the ferromagnetic structure in agreement with experiment.^{12,36}

The basal plane in LaTiO_3 undergoes the elongation in the direction of orthorhombic a -axis. It leads to such kind of orbital ordering then the orbitals of Ti ions placed in the ab -plane point almost along the same direction, but not to the oxygens (Fig. 4, left panel). Thus, this in-plane “ferroorbital ordering” implies large hopping integrals not only between two occupied (AFM interactions), but also between occupied and unoccupied (FM interactions) d -orbitals on different sites. The latter agrees with direct calculation of the exchange interaction parameters in Hartree-Fock approximation⁹ and have to be taken into account in model calculations.

The presence of a mirror plane in GdFeO_3 -type structure perpendicular to c -axis¹⁶ results in such kind of orbital ordering in c -direction that the lobes of the orbitals point to each other (see Fig. 5, left panel). This is in strong contrast to the orbital ordering in ab -plane, where orbitals are directed away from the oxygens.

The complicated orbital structure of LaTiO_3 does not favor the isotropic magnetic interactions in LaTiO_3 . But this is not a unique situation. It is generally accepted that YTiO_3 shows Jahn-Teller distortions and corresponding orbital ordering (Ref. 37 and references therein). Experimentally however it also has isotropic magnetic properties, which are hard to explain by orbital ordering. This would require an unrealistic set of parameters.¹⁴

Thus the isotropic character of exchange in both LaTiO_3 and YTiO_3 remains an open problem. Whether the orbital fluctuations^{10,14} with CF splitting of ~ 200 meV can resolve this problem, is not clear to us. Another option could be that the actual crystal (and consequently orbital) structure of LaTiO_3 is somewhat different from the accepted one - see the recent results in Ref. 38, where the indications of monoclinic distortions have been found. This question requires further investigations.

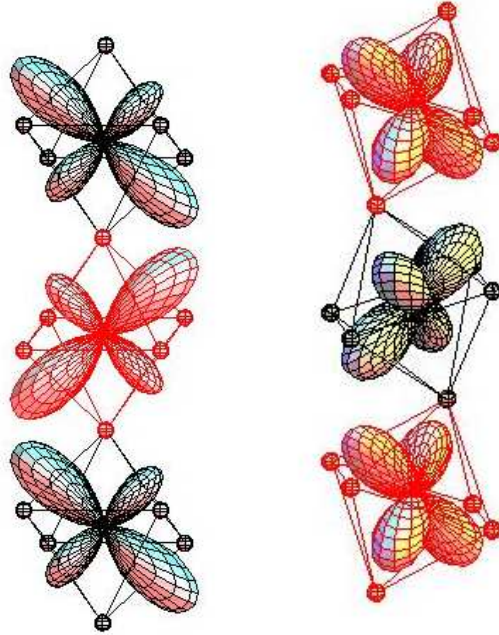


FIG. 5: (color online) Orbital ordering in LaTiO_3 (left) and YTiO_3 (right) in c -direction obtained in the framework of the LDA+U calculations for AFM-G and FM structures, respectively.

VIII. CONCLUSIONS

Following the logic of the present paper we would like to stress two general points.

(I) In the framework of LDA+U approximation we propose the *direct* method of calculation of crystal-field excitation energy. It can be useful for comparison with the results of spectroscopic measurements because it takes into account fast relaxations of electronic system. Any electron excitations in spectroscopy are accompanied by such relaxations and it should be definitely taken into consideration in the calculation of these excitations.

Moreover, this scheme is more reliable than others because it uses not eigenvalues of LDA but its total energies. In addition, the method does not have an ambiguity in the definition of the basis set as any projection or downfolding procedure does, because all states included in the Hamiltonian are used. The latter is especially important for low symmetry systems where it is not clear what kind of linear combination of d -wave function and in which coordinate system should be taken for construction of a few orbital tight-binding Hamiltonian.

(II) We probe this method on Y and La titanates, for which the value of crystal-field excitation energy is indeed essential. Using Wannier function projection of LDA full-orbital Hamiltonian it is found that CFS between the lowest and the next in energy t_{2g} level is 230 meV and 180 meV for La and Y titanates, in agreement with previous estimate.⁸

According to the results of present calculations, fast electronic relaxations reduce CFS by $\sim 30\%$ (it amounts to 70 meV in case of LaTiO_3) as compared with the difference of LDA one electron energies or CFS obtained by Madelung point charge summation.⁴ However, the value of crystal-field excitation energy is still large enough to make orbital liquid formation in titanates rather unlikely. At the same time the intricate orbital ordering in contrast to the expectations from the model calculations does not favor isotropic magnetic interaction in LaTiO_3 .

IX. ACKNOWLEDGMENTS

We would like to thank I.V. Solov'yev, D.E. Kondakov, M.A. Korotin, A.I. Poteryaev, S. Okatov and A.I. Lichtenstein for very useful discussion of calculation details. We also acknowledge fruitful communications with G. Khaliullin, M. Haverkort, M. Grüninger, M. Cwik, E. Müller-Hartmann, M. Braden and especially L.H. Tjeng. This work is supported by Russian Foundation for Basic Research under the grants RFFI-04-02-16096 and RFFI-03-0239024, Netherlands Organization for Scientific Research through NWO 047.016.005 and by the Deutsche Forschungsgemeinschaft through SFB 608.

-
- * Electronic address: streltsov@optics.imp.uran.ru
- ¹ J.B. Goodenough, *Magnetism and the Chemical Bond*, (Interscience publishers, New York-London. 1963).
 - ² C.J. Ballhausen, *Introduction to Ligand Field Theory*, (McGraw-Hill, New York, 1962).
 - ³ J.P. Elliott and P.G. Dawber, *Symmetry in Physics*, (Oxford University Press, New York, 1989).
 - ⁴ M. Cwik, T. Lorenz, J. Baier, R. Müller, G. André, F. Bourée, F. Lichtenberg, A. Freimuth, R. Schmitz, E. Müller-Hartmann, and M. Braden, *Phys. Rev. B* **68**, 060401(R) (2003).
 - ⁵ I.A. Nekrasov, S.V. Streltsov, M.A. Korotin, and V.I. Anisimov, *Phys. Rev. B* **68**, 235113 (2003).
 - ⁶ O.K. Andersen and T. Saha-Dasgupta, *Phys. Rev. B* **62**, R16219 (2000).
 - ⁷ V.I. Anisimov *et al.*, cond-mat/0407359.
 - ⁸ E. Pavarini, S. Biermann, A. Poteryaev, A.I. Lichtenstein, A. Georges, and O. K. Andersen, *Phys. Rev. Lett.* **92**, 176403 (2004).
 - ⁹ I.V. Solov'yev, *Phys. Rev. B* **69**, 134403 (2004).
 - ¹⁰ B. Keimer, D. Casa, A. Ivanov, J.W. Lynn, M.v. Zimmermann, J.P. Hill, D. Gibbs, Y. Taguchi, and Y. Tokura, *Phys. Rev. Lett.* **85**, 3946 (2000).
 - ¹¹ G. Khaliullin and S. Maekawa, *Phys. Rev. Lett.* **85**, 3950 (2000).
 - ¹² J.R. Hester, K. Tomimoto, H. Noma, F.P. Okamura, and J. Akimitsu, *Acta Cryst.* **B53**, 739 (1997).
 - ¹³ G.I. Meijer, W. Henggeler, J. Brown, O.-S. Becker, J.G. Bednorz, C. Rossel, and P. Wachter, *Phys. Rev. B* **59**, 11832 (1999).
 - ¹⁴ C. Ulrich, G. Khaliullin, S. Okamoto, M. Reehuis, A. Ivanov, H. He, Y. Taguchi, Y. Tokura, and B. Keimer, *Phys. Rev. Lett.* **89**, 167202 (2002).
 - ¹⁵ R. Schmitz, O. Entin-Wohlman, A. Aharony, A. B. Harris, and E. Müller-Hartmann, cond-mat/0407524.
 - ¹⁶ M. Mochizuki and M. Imada, *J. Phys. Soc. Jpn.* **73**, 1833 (2004).
 - ¹⁷ O.K. Andersen, *Phys. Rev. B* **12**, 3060 (1976).
 - ¹⁸ P. Blaha *et al.*, WIEN2k, An Augmented Plane Wave + Local Orbitals Program for Calculating Crystal Properties, Karlheinz Schwarz, Techn. Universität Wien, Austria, 2001.
 - ¹⁹ R.D. Shannon, *Acta Cryst.*, **A32**, 751 (1976).
 - ²⁰ A. Chainani, M. Mathew, and D.D. Sarma, *Phys. Rev. B* **46**, 9976 (1992).
 - ²¹ L.F. Mattheiss and D.R. Hamann, *Phys. Rev. B* **33**, 823 (1986).
 - ²² G.H. Wannier, *Phys. Rev.* **52**, 191 (1937).
 - ²³ N. Marzari and D. Vanderbilt, *Phys. Rev. B* **56**, 12847 (1997).
 - ²⁴ G.F. Koster, *Phys. Rev.* **89**, 67 (1953).

- ²⁵ W. Kohn, Phys. Rev. B **7**, 4388 (1973).
- ²⁶ Wei Ku, H. Rosner, W.E. Pickett, R.T. Scalettar, Phys. Rev. Lett. **89**, 167204 (2002).
- ²⁷ V.I. Anisimov, J. Zaanen, and O.K. Andersen, Phys. Rev. B **44**, 943 (1991).
- ²⁸ W.E. Pickett, S.C. Erwin, and E.C. Ethridge, Phys. Rev. B **58**, 1201 (1998).
- ²⁹ I. Solovyev, N. Hamada, and K. Terakura, Phys. Rev. B **53**, 7158 (1996).
- ³⁰ T. Mizokawa and A. Fujimori, Phys. Rev. B **54**, 5368 (1996).
- ³¹ A. Abragam and B. Bleaney, *Electron Paramagnetic Resonance of Transition Ions* (Oxford University Press, New York, 1970).
- ³² M.W. Haverkort *et al.*, Phys. Rev. Lett. **94**, 056401 (2005).
- ³³ M. Grüninger *et al.*, to be published.
- ³⁴ K.I. Kugel and D.I. Khomskii, Usp. Fiz. Nauk **136**, 621 (1982).
- ³⁵ D.A. MacLean *et al.*, J. Solid State Chem. **30**, 35 (1979).
- ³⁶ J. Akimitsu *et al.*, J. Phys. Soc. Jpn. **70**, 3475 (2001).
- ³⁷ H. Sawada, N. Hamada, and K. Terakura, Physica B, **237-238**, 46 (1997).
- ³⁸ M. Arao, Y. Inouem, and Y. Koyama, J. Phys. Chem. Solids **63**, 995 (2002).